Laboratory studies of the effect of cloud conditions on graupel/crystal charge transfer in thunderstorm electrification

By C. P. R. SAUNDERS[1]*, H. BAX-NORMAN[1], C. EMERSIC[1], E. E. AVILA[2] and N. E. CASTELLANO[2]

[1]*Centre for Atmospheric Science, The University of Manchester, UK*
[2]*FaMaF Universidad Nacional de Córdoba, Argentina*

SUMMARY

Collisions between vapour-grown ice crystals and a riming target, representing a graupel pellet falling in a thunderstorm, were shown by Reynolds, Brook and Gourley to transfer substantial charge, which they showed to be adequate to account for the development of charge centres leading to lightning in thunderstorms. Related experiments by Takahashi and Jayaratne *et al.* determined that the sign of charge transferred is dependent on the cloud liquid water content and on cloud temperature. There are marked differences between the results of Takahashi and Jayaratne in the details of the dependence they noted of the sign of graupel charging on cloud water and temperature. More recently, Pereyra *et al.* have shown that results somewhat similar in form to those of Takahashi are obtained by modifying the experimental technique used to prepare the clouds of ice crystals and supercooled water droplets used in the experiments.

In order to help resolve the reason for the differences in charge transfer results in various studies, work has continued in the Manchester laboratory with a modified cloud chamber in which the cloud conditions of the crystals and droplets may be controlled independently. Results indicate a profound effect on the charge sign of the particle growth conditions in the two clouds involved. For example, by suitable adjustments to the water contents of the two clouds, graupel is charged negatively by rebounding ice crystal collisions at higher cloud water contents than have been noted previously. It is suggested that the most important influence on charge sign is the relative diffusional growth rate of the two ice surfaces at the moment of impact and that this is affected by an increase in cloud supersaturation experienced by the ice crystals during the cloud mixing process just prior to collision. A range of cloud conditions is used in the present work in order to help determine the reasons for the various results reported previously.

Examination of some thunderstorm observations in the context of the present results points to the importance of mixing on the sign of the charge transferred during particle collisions when two cloud regions of different histories mix together.

KEYWORDS:　Cloud supersaturation　Ice crystal growth　Thunderstorm charging

1. INTRODUCTION

There is strong evidence from lightning studies and in-cloud measurements that the charge centres in thunderstorms are located in regions where the ice phase may be actively involved in the electrification process (Reynolds and Neill 1955). Reynolds and Brook (1956) noted rapid vertical development of the radar echo from precipitation just before the first lightning stroke. Krehbiel (1986) brought together many observations worldwide to show that the negative charge centre in most thunderstorms is located typically between the -10 and $-20\,°C$ temperature levels and remains at this level through the active period of storm electrification, while the upper positive charge region is carried aloft in the storm updraught. Illingworth and Lees (1992) observed the position of lightning and precipitation in a UK summer thunderstorm and confirmed that lightning is co-located with the maximum precipitation radar echo; they concluded that the presence of graupel is required for lightning to occur. López and Aubagnac (1997) studied an Oklahoma hailstorm with a well-organized supercell and observed the development of graupel coincident with cloud-to-ground lightning activity, which they attributed to negative graupel particle charging at $-15\,°C$. Observations within thunderstorms by Dye *et al.* (1986, 1988) confirmed that suitable cloud conditions for electrification occur in regions where supercooled water droplets, ice crystals and graupel

---

pellets coexist and that charging may be taking place along the updraught/downdraught interface. Consistent with these various observations is a possible thunderstorm charging process involving collisions of ice crystals with riming graupel pellets, first suggested by Reynolds *et al.* (1957). In laboratory studies, they grew ice crystals in a cloud of water droplets in a temperature-controlled chamber, then moved a target representing a graupel pellet through the mixed cloud while charge transferred to the target was measured. At a temperature around $-25\,^\circ$C, substantial negative charge was transferred to the graupel target while the rebounding ice crystals removed an equal and opposite positive charge. They suggested that the typical thunderstorm charge dipole is generated by the physical separation of graupel and ice crystals in the storm updraught. Subsequent laboratory studies by Takahashi (1978) and Jayaratne *et al.* (1983) confirmed that charge transfer is associated with ice crystal rebounds from riming graupel. They showed that the sign of the charge transfer is a function of the cloud temperature, T, and liquid water content, *LWC*, with the generation of negatively charged graupel at certain values of T and *LWC*, while at higher temperatures or higher values of *LWC*, graupel charges positively. This positive charging of graupel permits an explanation of the observations of a lower positive charge centre in thunderstorms, while the negatively charged ice crystals are carried in the updraught to reinforce the negative charge centre. This tripole structure has been discussed by Williams (1989), while more complicated charge structures have been reported by Stolzenburg *et al.* (2001). Recent observations by Rust and MacGorman (2002) and Rust *et al.* (2005) suggest the possibility of an inverted polarity dipole in some severe storms; this situation also needs to be accounted for by the dependence of charge sign on the microphysics of the cloud and particle conditions in various regions of thunderstorms where electrification takes place.

Jayaratne and Saunders (1985) and Brooks *et al.* (1997) realized that the accretion of rime on the graupel surface influences the charge transfer, so that the effective liquid water content, *EW* (the accreted fraction of the *LWC*), is more meaningful than the *LWC* by itself. The charge-sign boundaries on an *EW* vs. T plot from the studies by Takahashi (1978), Takahashi and Miyawaka (2002) and Saunders and Peck (1998), who developed the work of Jayaratne *et al.* (1983) and Saunders *et al.* (1991), are shown in Figure 1. Although the differences between the charge-sign reversal lines are apparent, there is agreement with Reynolds *et al.* (1957) that negatively charged graupel is to be expected at lower temperatures and at values of *EW* representative of thunderstorm conditions. The reasons for the different locations of these reversal lines on *EW* vs. T graphs has been the source of continued investigations and may be associated with differences in the experimental conditions in the laboratory studies. A resolution of this issue is important because the objective of laboratory simulations is to model nature as closely as possible in order to draw meaningful conclusions from the studies and to apply the results to real thunderstorms.

Studies by Gaskell and Illingworth (1980) and by Avila and Caranti (1994), in which falling 100 μm ice spheres rebounded from a riming target, also showed that the rimer charge sign reversed to negative at lower temperatures, thus revealing some similarities in the charging mechanism and indicating that the charge transfer is not a function of the special characteristics of ice crystals. Indeed, Jayaratne *et al.* (1983) found no difference in charge transfer results when they used plate or columnar ice crystals.

The above studies led each of the authors to suggest possible charge transfer mechanisms during particle collisions and rebounds; a common feature is the removal by one particle of part of the charged surface of the other particle, as proposed by Takahashi (1978). Baker *et al.* (1987) suggested that the relative diffusional growth rates (RGR) of
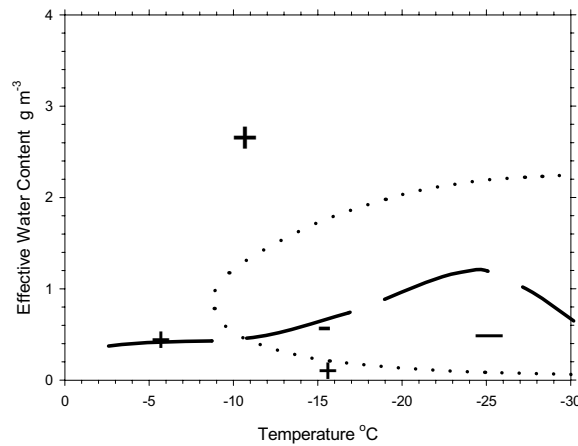
Figure 1. Charge sign boundaries. + Positive graupel above the upper boundaries. − Negative graupel below the upper boundaries. Saunders and Peck (1998) — — —. Takahashi (1978) . . . . Takahashi (2002) specific results at the three values of EW and T indicated; small + −.

the interacting ice surfaces would lead to the positive charging of the surface growing faster by vapour diffusion: the ice crystals and graupel surfaces grow by diffusion from the surrounding cloud whereas the graupel also grows from vapour released from the supercooled droplets freezing on the riming surface. So, droplet accretion rates and temperature-dependent droplet freezing times lead to surface differences that control the rate of growth and the sign of the charge transfer.

Williams *et al.* (1991) pointed out that in the process of accretion, graupel particles are heated by the release of latent heat from freezing droplets, so that at a sufficiently high rate of accretion the ice surface will sublimate. They associated this sublimation condition with negative charging of the rimer, which is consistent with the relative growth rate hypothesis when the ice crystals are growing in a supersaturated environment. Experiments by Magono and Takahashi (1963), Avila *et al.* (1995, 1996) and Saunders *et al.* (1999a) showed that the artificial heating of a riming target could lead to it charging negatively during collisions with ice crystals; the heating reduces the diffusional growth rate below that of the ice crystals.

Saunders *et al.* (2001) considered the effects of local supersaturation on the relative growth rates of the interacting surfaces in order to account for the charge-sign zones in Fig. 1. They found that by directing a stream of moist air towards a negatively charging graupel target, its charge sign could be reversed to positive during ice crystal rebounds. They also noted that mixing moist air into the ice crystal cloud strengthened the negative charging of the target. Both results are consistent with the RGR hypothesis and lead to the conclusion that the supersaturation in the cloud plays an important role in determining the charge sign through its influence on the growth rates of the interacting ice surfaces.

The positive charging of graupel at high values of EW presents a problem to the RGR hypothesis. The analysis of Williams *et al.* (1991) showed that the high accretion rates occurring at high LWC lead to sufficient rime heating to cause sublimation, so that negative rimer charging would be expected at accretion rates up to the wet growth limit. However, the sign of graupel charging is positive at high values of EW as shown in Fig. 1; the wet growth limit is at even higher values of EW than these charge-sign reversal lines (see Fig. 2). Recent analysis by Mitzeva *et al.* (2005) has pointed out
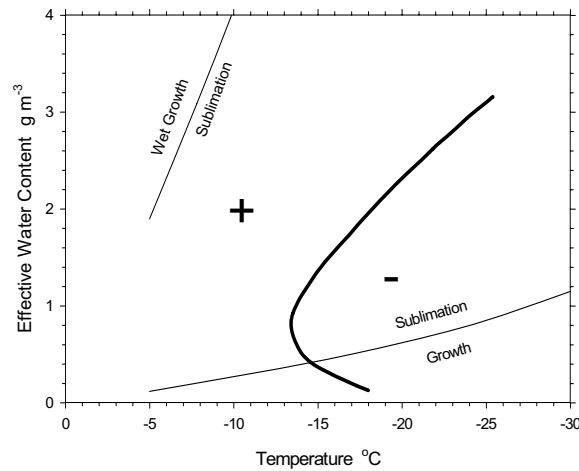
Figure 2.   Graupel charge-sign boundary from Pereyra *et al.* (2000) and rimer growth state boundaries.

that in the original concept of the significance of relative growth rates by Baker *et al.* (1987), most of the vapour from droplets freezing on the rimer at 0 °C was assumed to be directed away from the droplets; only vapour emitted tangentially to the colder rimer surface was captured. The new calculations showed that when account is taken of vapour flow directed initially away from the freezing droplet surface but then returning to the colder rimer surface under the influence of the temperature-dependent vapour pressure difference, the rimer diffusional growth can exceed that of the ice crystals, causing it to charge positively at high values of *EW*.

In the experiments performed in Manchester by Jayaratne *et al.* (1983), Keith and Saunders (1990), Saunders *et al.* (1991), Brooks *et al.* (1997) and Saunders and Peck (1998), the ice crystals, supercooled droplets and the riming target were all located in the same cloud. The cloud chamber was large enough for the ice crystal growth conditions to be stable, as shown by the steady values of *EW* obtained in the studies of Keith and Saunders (1990), who determined *EW* by measuring the heat rise of the riming target. The mixed cloud of crystals and droplets was drawn past the target while charge transfer due to crystal rebounds from the accreted rime was measured. Takahashi (1978) also used a chamber with similar crystal concentrations and liquid water contents, so there was no apparent difference between the cloud conditions in these sets of experiments that could account for the differences noted in Fig. 1. However, Pereyra *et al.* (2000) used separate chambers for the production of their ice crystals and droplets; the two clouds were mixed shortly before the cloud particles collided with the target. Their results are shown in Fig. 2 together with lines showing the boundaries between diffusional growth, sublimation due to rime heating, and wet growth of the rimer determined from the rimer heat analysis of Macklin and Payne (1967). The graupel charge-sign boundary obtained by Pereyra *et al.* (2000) is similar in form to that of Takahashi (1978), shown in Fig. 1. The boundary lines showing the growth state of the graupel do not coincide with the charge-sign boundaries, indicating no simple explanation of charge sign in terms of the growth or sublimation state of the rimer surface alone.

Because of our earlier laboratory results showing the influence of cloud supersaturation on charge sign, and experiments showing differences between laboratory results

using single or separate cloud chambers, the present study is designed to examine the influence of the particular experimental techniques used on the sign of charge transferred during crystal/graupel rebounding collisions. In the earlier experiments conducted in Manchester, a single cloud chamber was used in which the ice crystals and droplets involved in the riming process were well mixed before the cloud was drawn past the target. The present investigation uses two separate cloud chambers for the growth of the ice crystals and droplets, and studies the effect on charging when the two sets of cloud particles are mixed together just prior to impact on the target.

2. THE EXPERIMENTS

The study is into the effect on the sign of charge transferred to riming graupel during ice crystal interactions when the crystals and riming droplets are grown in separate cloud chambers. The Manchester cloud chamber, with temperature control down to $-30\,°C$, used in our previous studies of charge transfer with a single chamber for both droplet and crystal growth, is now divided into two separate chambers each of height 2 m and floor area 1×0.75 m^2 (Figure 3). The divider is a sheet of plastic thin enough to permit good thermal contact between the two chambers. Water vapour is provided continuously by two boilers whose power outputs are controlled in order to obtain the required liquid water contents in the chambers. The boilers run for about ten minutes before the experiments start so that the condensed droplets supercool and have time to come to steady values of liquid water content in each cloud, as shown by measurements of rime accretion and by particle imaging probes sampling the cloud. Ice crystals are then nucleated in one chamber by introducing a fine metal seeding wire previously cooled in liquid nitrogen. The concentration of ice crystals produced is controlled by the seeding time, which is 2 to 3 s for a 'long' seed and about 0.5 s for a 'short' seed. The seeding process is manual and good reproducibility of the crystal cloud produced is readily achieved with practice. The crystals grow from the droplets and the available vapour, whose supply to the crystal chamber is continued throughout the experiment in order to maintain ice supersaturation. After 2 min the visibility in the crystal cloud (illuminated with a spotlight and viewed through a window in the cloud chamber from outside the cold room) increases as the droplets evaporate while the crystals grow. An external air pump is then switched on for 30 s to cause the separate clouds of crystals and droplets to mix and flow past the riming target.

The airflow speed in earlier studies in Manchester was 3 m s^{-1} representing the fall speed of small graupel pellets. The studies of Takahashi (1978) used a speed of 9 m s^{-1} with a moving rod target while his studies in 2002 used both 3 and 9 m s^{-1} with levitated targets. The present work is carried out at a speed of 6 m s^{-1}, representative of the fall speed of graupel pellets of a few millimetres diameter (Heymsfield and Kajikawa 1987). Figure 3 shows how the droplet and crystal clouds are brought together, then pass through a 14 cm long tube on the way to the target, giving a mixing time of 23 ms. The Reynolds number of around 19 000 indicates that the flow is in the turbulent regime thus ensuring good mixing between the two sets of cloud particles.

The rimer, representing a graupel pellet, is a brass rod of diameter 3 mm connected to an electrometer amplifier that measures the charging current from the many crystal/graupel charge transfers during rebounding collisions. A rod target is used for experimental convenience rather than a sphere: our previous work has shown that the charge transfers to a riming surface are not affected by the shape of the substrate. Because the charging current is low, the amplifier is mounted directly on the target rod in order to prevent microphonic noise associated with slight movements of long cables. The target

Plan View of the Manchester Cloud Chamber

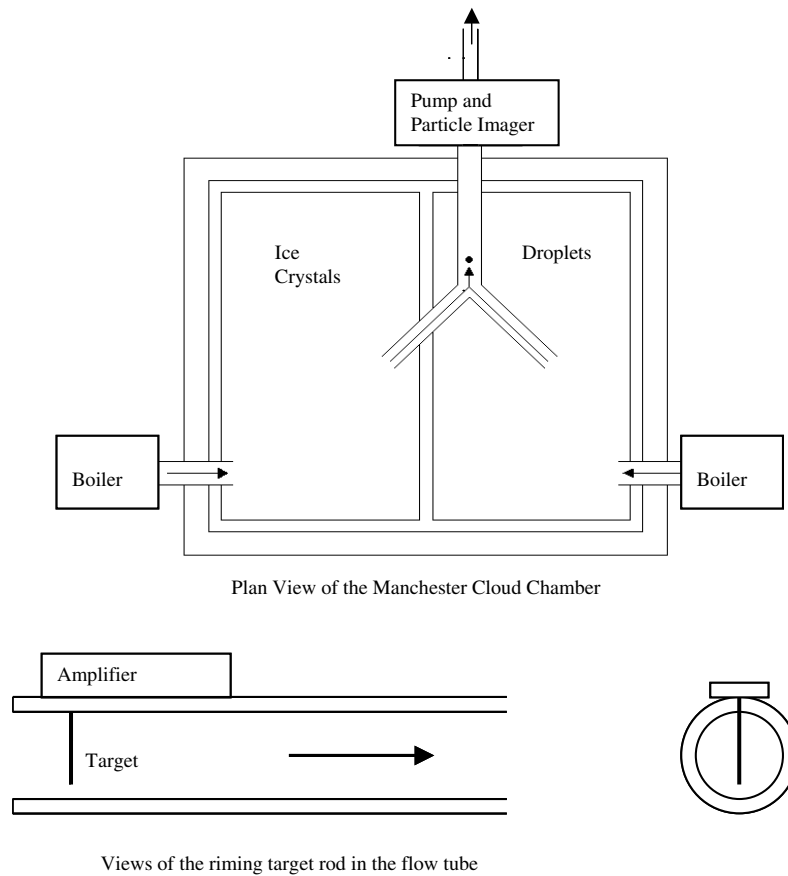Views of the riming target rod in the flow tube

Figure 3. The cloud chambers and target.

rod is easily removed in order to study and weigh the accumulated rime ice. Downwind of the target, the cloud particles pass through a cloud particle imager, CPI, (Stratton Park Engineering Company, USA) to obtain an indication of particle size distributions. Temperatures in the cloud chambers are measured with platinum resistance thermometers and thermocouples giving mean cloud temperatures to within ± 1 degC.

In preliminary experiments, the initial effective water content of the droplets in the ice crystal chamber before seeding is determined by drawing the droplets past the target rod and weighing the target plus accumulated rime. Two values of *EW* used extensively in this work, adjusted by the power to the boiler, are 0.2 g m^{-3} and 0.3 g m^{-3}. These values of *EW* are set sufficiently low to ensure that crystal growth depletes the droplets, despite the continued provision of water vapour, so that the droplets will be too small to accrete on the rimer, leading to a measured *EW* from collected ice crystals alone of less than 0.05 g m^{-3}. Thus, following mixing of the crystals with the separate droplet clouds, the accreted water on the target comes principally from the droplet cloud. The rime accreted on the target is weighed in all the mixed cloud experiments in order to determine the values of *EW* presented in the figures to follow.

The CPI data permit an analysis of the rate of growth of the crystals at the time of the charge transfer experiments and make possible a determination of the
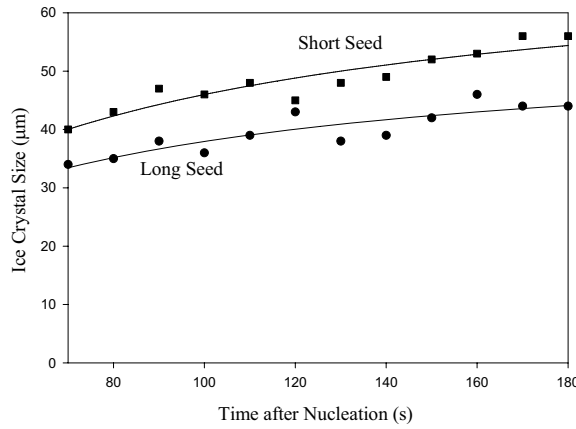
Figure 4.   Ice crystal size against time since crystal nucleation at −15 °C.
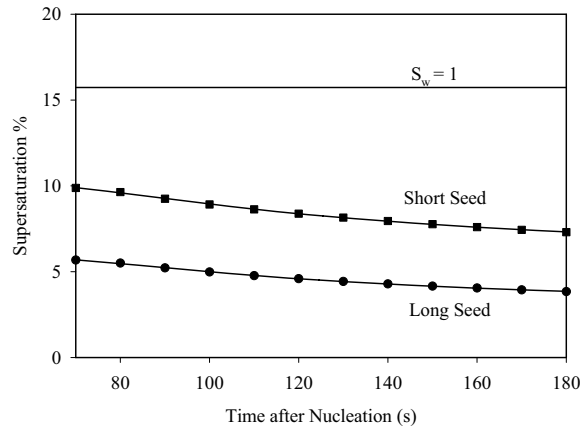

Figure 5.   Percentage supersaturation over ice against time since crystal nucleation at −15 °C.

cloud supersaturation as a function of nucleation technique. For a cloud temperature of −15 °C, the standard ice crystal diffusional growth equations are applied with the assumption that the ice crystals are spherical; tests with various shape factors showed that crystal shape is not significant here. Using the modal crystal sizes from the data, Fig. 4 indicates ice crystal growth for both seeding techniques with an initial *EW* of 0.2 g m^{-3}. Figure 5 indicates the calculated supersaturations determined from the growth rates for size increases in 10 s intervals using the best-fit lines shown in Fig. 4. The use of incremental crystal size measurements in this calculation overcomes the absolute sizing limitations of the CPI probe. The line for water saturation at −15 °C ($S_w = 1$) confirms that the ice crystal cloud was undersaturated with respect to water. Continued crystal growth for both short and long nucleation times shows that the crystal cloud remains supersaturated with respect to ice so that the crystals are growing in the ice chamber when they start their journey to the target, approximately 120 s after seeding the cloud. The longer seed time produces the lower value of supersaturation because competition for vapour in the chamber increases with larger numbers of crystals.
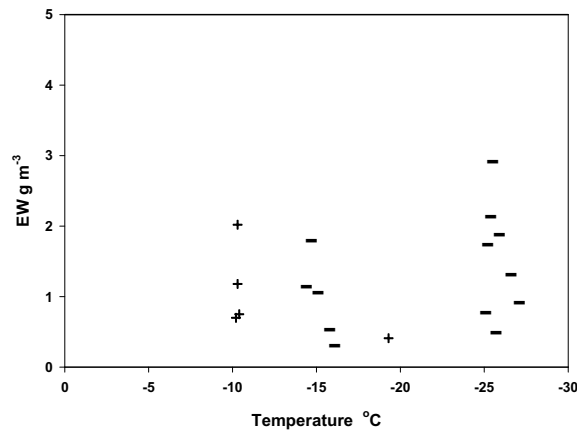
Figure 6. Rimer charge sign as a function of Effective Water content and temperature with ice crystals grown in conditions of high competition for vapour.

3. RESULTS

Initial studies carried out at cloud temperatures around $-15\,^{\circ}$C indicated that the sign of charging of the rimer is responsive to the ice crystal growth conditions. The results shown in Figure 6 were obtained with initially low crystal growth rates, obtained by limiting the vapour supply to the crystal cloud, followed by mixing with the droplet cloud. The figure shows negative charging of the target at $-15\,^{\circ}$C for values of *EW* up to 2 g m^{-3}, which is a higher value of *EW* for negative graupel charge than has been obtained in this laboratory using a single cloud technique in previous experiments.

Figures 7, 8 and 9 show the effect on the ice crystal cloud of varying the initial values of water content and the seeding time in the crystal chamber. By providing more vapour and a long seeding time, a high ice crystal concentration is produced, Fig. 7. The largest crystals are produced with a high initial water content and a short seed that produces fewer crystals which benefit from reduced competition for the available vapour, Fig. 8. Limiting the vapour supply leads to reduced crystal sizes, Fig. 9. Figure 10 shows a typical droplet distribution from the droplet cloud chamber alone, which is representative of that in all the experiments. The droplet diameters extend to 50 μm, while the CPI small particle size cut-off around 10 μm is evident. The CPI sizing error has been studied in the Manchester laboratory; the maximum error for 50 μm particles is below 23% (Connolly, private communication). The initial droplet spectrum in the ice crystal chamber before nucleation is similar to that in the droplet cloud.

A long series of experiments was performed in which the droplet cloud was adjusted to give values of *EW* in the range up to about 4.5 g m^{-3} while the ice crystal cloud experienced a low vapour supply in which cloud conditions remained between ice saturation and water saturation, as discussed below. Figure 11 shows the rimer charge sign as a function of *EW* and cloud temperature from experiments in which the value of *EW* in the initial crystal cloud before seeding is 0.3 g m^{-3} with a short seed. It is clear that negative charging of the target extends to very high values of *EW* sourced from the droplet chamber. However, the highest temperature at which the riming target charges negatively is around $-15\,^{\circ}$C, which is similar to the value obtained by Pereyra *et al.* (2000) but does not match the value of around $-10\,^{\circ}$C obtained by Takahashi (1978). Given indications that the growth condition of the ice crystals is important in
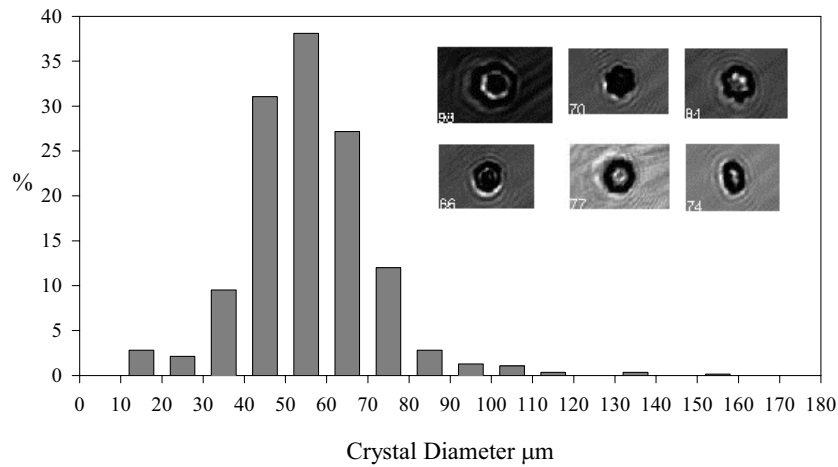
Figure 7. Ice crystal size distribution from an initial $EW = 0.3$ g m^{-3} following a 'long' seed. Images from the CPI show crystals around 80 μm diameter.
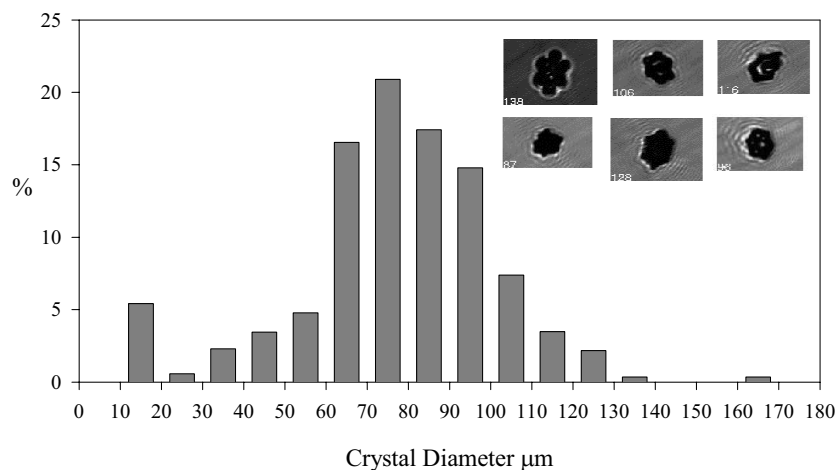

Figure 8. Ice crystal size distribution from an initial $EW = 0.3$ g m^{-3} following a 'short' seed. The CPI images show crystals between 90 and 140 μm diameter.

controlling the sign of charging, a further set of experiments was conducted with an initial EW in the crystal cloud of 0.3 g m^{-3}, but the seeding technique was changed to a long seed to increase the competition for vapour among the growing ice crystals. The result was that negative charging occurred at temperatures as high as $-12\,^\circ$C under these conditions. The experiments were continued using a value of EW in the crystal chamber of only 0.2 g m^{-3} with a short nucleation time that also limited the vapour supply to the growing crystals. The results were similar to the previous dataset and so both sets of results are shown together in Figure 12. The boundary between the positive and negative zones, based on the dataset presented in Fig. 12, is shown in Figure 13 together with charge-sign boundary lines from other studies.

Continuing the search for high-temperature negative charging, a series of experiments was performed at an initial EW of 0.2 g m^{-3} for crystal growth but with a long
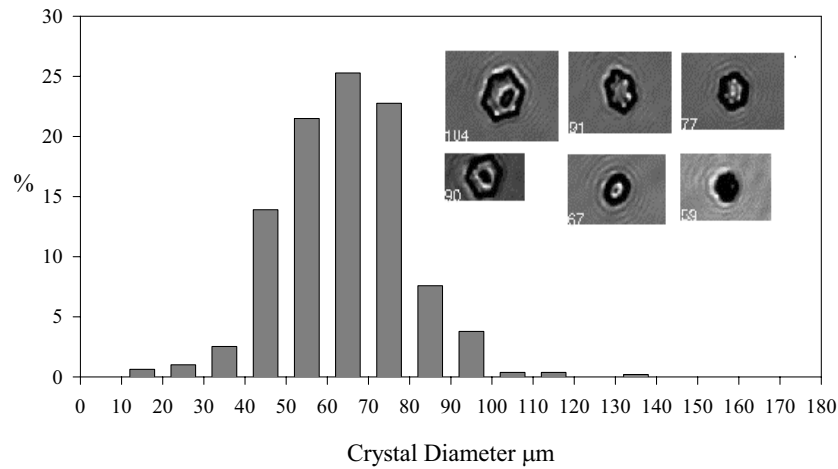
Figure 9. Ice crystal size distribution from an initial $EW = 0.2$ g m^{-3} following a 'short' seed. The crystal images are between 60 and 100 μm diameter.
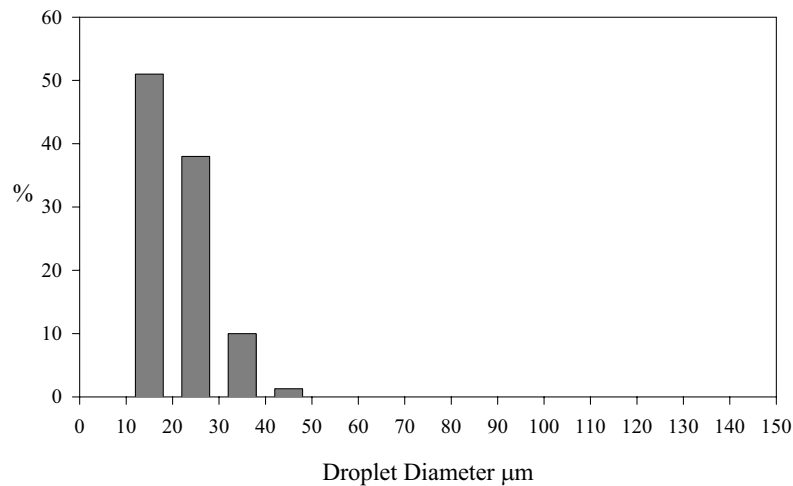

Figure 10. Range of cloud droplet sizes produced at $-18\,^{\circ}$C.

seed and simultaneous reduction of the vapour supply to the crystals to zero. The crystal spectrum shows a reduced size range compared with Figs. 4 and 5 with a peak in the size distribution at 40 μm. A similar distribution of positive and negative charge transfers to Fig. 10 was noted but with negative rimer charging at $-10\,^{\circ}$C for a cloud EW of 1 g m^{-3}.

In the next series of experiments the ice crystal cloud was seeded continuously at an initial EW of 0.3 g m^{-3} with the water vapour supply removed at the time of nucleation. An open dewar of liquid nitrogen in the crystal chamber was stirred slightly in order to continuously nucleate the cloud and produce a high concentration of crystals. The effect on crystal size was to shift the distribution to smaller sizes, the distribution peaking at 20 to 30 μm due to the enhanced competition for vapour. In addition, the details of the vapour supply to the droplet cloud were changed: rather than having a steady cloud produced over 10 minutes, a higher boiler power was used for a few minutes before
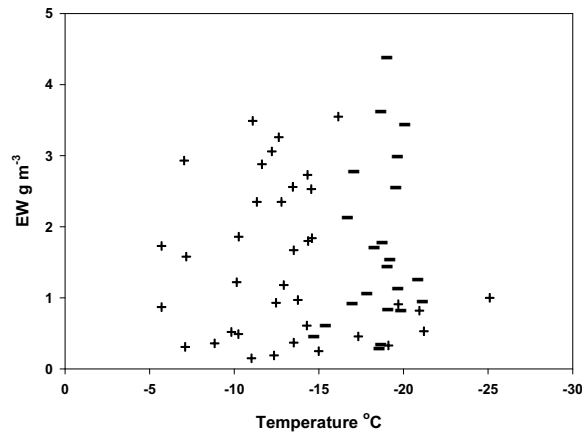
Figure 11. Rimer charge sign as a function of Effective Water content and Temperature with ice crystals grown in an initial EW of 0.3 g m^{-3} following a 'short' seed.
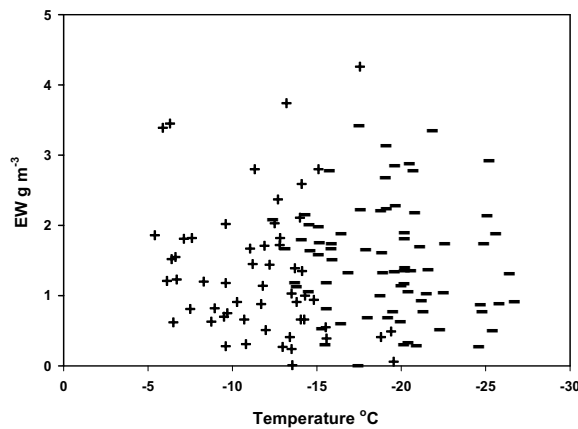

Figure 12. Rimer charge sign as a function of Effective Water content and Temperature with ice crystals grown in conditions of limited vapour supply, either an initial EW of 0.3 g m^{-3} following a 'long' seed or an initial EW of 0.2 g m^{-3} following a 'short' seed.

mixing the clouds in order to increase the supersaturation experienced by the crystals on mixing. The resulting charge transfer data showed negative charging at a maximum temperature of $-7.7\,°C$ for an EW of 1.7 g m^{-3}. This last case examined has similarities in technique to the experiments of Takahashi (1978) who seeded the crystals in the cloud chamber continuously and directed a freshly produced supercooled droplet stream at the riming target; he obtained negative charging at $-7\,°C$ at an EW around 1 g m^{-3}.

From the preceding experiments, it seems that reducing the rate of growth of the crystals, prior to mixing, promotes negative charging of the target. Experiments were performed to test whether this effect could be overcome by introducing more vapour to the crystal cloud. Ice crystals grown at $-15\,°C$ in a reduced vapour supply were subjected to an increased vapour supply for 15 s before cloud mixing. Under these conditions, the target charged positively.
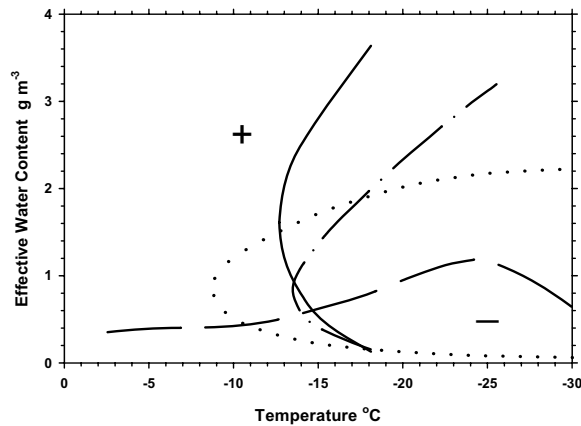
Figure 13. Rimer charge sign boundaries for the present work (based on the data shown in Fig. 10) and earlier studies. ———— Present results. ——— · ——— Pereyra, Avila, Castellano and Saunders (2000). . . . . Takahashi (1978). — — — Saunders and Peck (1998).

4. DISCUSSION

(*a*) *Effects of crystal growth conditions on charging*

Figure 13 provides a comparison of the positive and negative charge transfer zones obtained in this and earlier studies. There are obvious differences between the new and the earlier results obtained in Manchester, with results from other laboratories coming between the two extremes. The new results obtained here with two separate cloud particle growth chambers have produced a charge-sign reversal line at very high values of *EW*. The experiments involved controlling the vapour supply to the ice crystal cloud either by limiting the vapour available at the time of ice crystal nucleation and/or by controlling the seeding time. Figures 7, 8 and 9 show the resulting ice crystal distributions in these cases.

Considering the new results first, a considerable difference exists between the supersaturations experienced by the two sets of cloud particles before mixing the droplet and crystal clouds together on the way to the target. The ice crystal cloud is below water saturation and above ice saturation, as shown by the continued growth of the crystals confirmed by the CPI data analysis shown in Figs. 4 and 5, while the droplet cloud is near to water saturation having a continuous supply of vapour. In all cases the droplet and crystal clouds are at the same temperature because the wall between the chambers is thin and permits good heat transfer. The results point to the importance of the vapour supply to the ice crystals during their growth in influencing the subsequent charge transfer following mixing with the droplet cloud.

The analysis of growth rates and supersaturation leads to a possible explanation of the dependence of the position of the charge-sign reversal line on the growth conditions of the ice crystals. Growing ice crystals are heated by vapour deposition that releases latent heat and, in turn, the heat reduces the vapour deposition rate. In the present crystal growth chamber, the ice crystals grow slower than they would have done in a cloud at water saturation and so are colder because of the reduced rate of vapour deposition. The result is that upon mixing with the droplet cloud at water saturation, the crystals experience an increased supersaturation that causes an increase in their growth rate. On collision with the rimer, faster growing crystals charge more strongly positive leading

to negative charging of the target in accord with the relative growth rate concept and in agreement with the measurements reported here.

The enhanced crystal growth during mixing is transient and lasts while the crystals are heated by their increased vapour supply. Castellano *et al.* (2004) calculated that for the present experimental set up, with a mixing time of 23 ms, there is insufficient time for all but the smallest crystals to heat up to the new temperature appropriate to their new growth rate. Thus for crystals larger than about 20 μm, which because of the strong dependence of charging on crystal size (Keith and Saunders 1990) are the crystals responsible for the measured charge transfers, there is adequate time for the charge sign to be affected by the transient high growth rate.

(*b*)   *Effect of ice crystal size*

An alternative explanation for the observations in the present study may be associated with ice crystal size. When the ice crystals grow in a reduced vapour supply they are smaller than they would normally have been at the time of the charge transfer experiments. Standard theory tells us that the growth rate is inversely proportional to crystal size so that smaller ice crystals grow faster. Upon mixing into the droplet cloud with its higher supersaturation, the smaller crystals would grow fast leading to enhanced negative charging of the rimer. The experiment described at the end of section 3, in which vapour was reintroduced to the ice crystal cloud for 15 s following the usual reduced growth rate conditions, caused reversal of the expected negative rimer charging to positive. This time is not long enough for the crystals to significantly increase their size but is sufficient for the increased growth rate to increase their temperature, so that on mixing with the droplet cloud, transient enhanced growth did not take place. The result indicates that the observed enhanced negative charge transfers were not simply caused by the crystals being small. This experiment also confirms that the effect of reducing the crystal growth rate, resulting in negative charging of the target, can be reversed by the reintroduction of vapour to the crystal cloud.

(*c*)   *Considerations of velocity and the rate of rime accretion*

Previous charge transfer studies in Manchester by Saunders *et al.* (1991) were performed at 3 m s^{-1} in order to match the fall velocity of small graupel pellets. In those experiments, the target moved through the cloud or the cloud was drawn past a stationary target, both methods giving similar results. The charge-sign reversal line on an *EW* vs. *T* graph indicated a change from negative to positive graupel charging on increasing *EW*. In order to be able to relate this reversal line to higher velocities, *V*, corresponding to the fall speeds of graupel of a few millimetres diameter, Brooks *et al.* (1997) used the Rime Accretion Rate as the variable, where *RAR* = *EW* × *V*, rather than *EW*. The amount of accretion and rime heating for a constant *RAR*, which influences the sign of charging, is approximately the same if *V* is doubled and *EW* halved for example (the droplet collection efficiency, *E*, changes slightly with velocity in the range of interest). The charge-sign experiments of Saunders and Peck (1998) were performed at several velocities in the range 3 to 14 m s^{-1} and were presented in that paper in terms of a critical charge-sign reversal line on a plot of *RAR* vs. *T*. For reasons discussed below, Fig. 13 is presented in terms of an *EW* vs. *T* plot and the reversal line from Saunders and Peck shown there has been converted from *RAR* to *EW* for a speed of 3 m s^{-1}. This reversal line is in agreement with that of Saunders *et al.* (1991) down to −25 °C and extends it with measurements down to −30 °C. The reversal line shown on Fig. 13 from Takahashi (1978) was obtained at 9 m s^{-1} while the line from Pereyra *et al.* (2000) was obtained at 8.5 m s^{-1}.

Consideration of the velocities used for each of the charge reversal lines shown in Fig. 13 indicates that the effect of plotting *RAR* vs. *T* rather than *EW* vs. *T* would have brought the positive slope portions of the reversal lines of Takahashi and of Pereyra *et al.* closer together, but would have moved the Saunders and Peck line further from the others. This points to the concept of using *RAR* as a good one but it may be applied only to results obtained under similar circumstances. For example, the various reversal lines obtained in two-cloud mixing experiments may be brought into self-agreement, while the results of Saunders and Peck (1998) obtained over a range of velocities in one-cloud experiments may also be brought into self-agreement. However, one-cloud and two-cloud datasets cannot be rationalized in this way. The conclusion is that there is a fundamental difference between the microphysics in the one and two-cloud cases possibly connected with the availability of vapour to the growing ice crystals. In the one-cloud case, the crystals are growing in the same cloud as the riming target and so experience no transient conditions on the way to the target, whereas in the two-cloud case, the vapour-deprived crystals experience an enhanced diffusional growth on mixing with the droplet cloud that favours negative rimer charging.

(d)   *Effect of droplet size on charge transfer*

Although in the present experiments the droplet cloud was not affected by changes to the crystal growth conditions, droplet size is known to influence the charge transfer through various effects and so needs to be representative. Korolev *et al.* (2001) found droplets in cumulus ranged up to 100 μm diameter with an effective peak diameter at 12 μm. Heymsfield and Hjelmfelt (1984) measured water contents and droplet size distributions in Oklahoma convective clouds; for *LWC* between 1.5 and 2 g m^{-3} the volume-weighted droplet diameter was 20 μm with the range extending to 50 μm. Williams and Zhang (1996) reported volume-weighted droplet diameters in the range 12 to 26 μm from various severe-storm studies. Dye *et al.* (1989) measured mean diameters of 15 to 20 μm, up to 40 μm in New Mexico storms. Blyth and Latham (1993), also in New Mexico, reported mean diameters of 20 to 50 μm. Willis *et al.* (1994), in a summertime convective cloud in Florida, found droplets ranged up to 40 μm with peak diameters around 20 μm. Heymsfield (1982) noted, in high-plains summer storms, for a *LWC* of 1 g m^{-3} the mean droplet diameter was 16 μm; for *LWC*s of 0.5 and 2 g m^{-3} the mean droplet sizes were 14 and 18 μm respectively. Thus the present droplet distribution up to 50 μm shown in Fig. 8 is representative.

Our preference for using *EW* rather than *LWC* is because the charge transfer is influenced by rime accretion. Jayaratne and Saunders (1985) found that a rimer could charge positively or negatively for the same *LWC* depending on droplet size because the accretion rate is affected by the graupel/droplet collision efficiency, which is a function of droplet size. Charge-sign reversal from negative to positive on increase in *EW* occurs when the effects of heating, favouring negative charging, and vapour flux to the rimer surface from freezing droplets, favouring positive charging, are in balance (Mitzeva *et al.* 2005). This does mean that numerical models of thunderstorm electric field development by the *EW*-dependent crystal/graupel charging mechanism have to take into account the decrease of rimer/droplet collision efficiency with decreasing droplet size and increasing rimer size.

In one-cloud experiments with small supercooled water droplets of mean diameter below 4 μm, Jayaratne (1998a) noted enhanced negative rimer charging during crystal rebounds at temperatures around $-10\,^{\circ}$C. Saunders *et al.* (1999b) also showed that charge-sign reversal moved to higher values of *EW* when the mean size of the droplets was reduced. They attributed this effect to increased vapour diffusion to the crystals

from near-field droplet sources in the cloud, following Marshall and Langleben (1954) whose theory was recently confirmed by Castellano *et al.* (2004). In the present study the droplet cloud size distribution is realistically broad and is not a variable.

In the present work the droplet size distribution in the droplet chamber is broader than that experienced in the one-cloud experiments because there has been no depletion of vapour by crystal growth. The 'one-cloud' droplet spectrum used by Jayaratne *et al.* (1983) extended to 30 μm, while in the present work the droplet sizes reach 50 μm. Avila *et al.* (1998, 1999) showed that the presence of larger droplets in one-cloud experiments can favour negative rimer charging; they attributed this result to the longer freezing time of larger droplets on the target permitting spreading during freezing and so providing a smoother rime surface; the resulting decreased ventilation causes heat retention, promoting negative rime charging. However, this effect only increased the critical value of *EW* for charge-sign reversal by a fraction of a gram per cubic metre, which is small compared with the effects of mixing described here. Also, Takahashi (1978) found no effect of droplet size on charge transfer with droplet spectra extending to diameters over 100 μm.

Droplet size also has an effect on rime density; Macklin (1962) showed that larger droplets, higher velocity and higher temperatures favour increased rime density. Williams and Zhang (1996) suggested that rime density increase with velocity may influence charge transfer; however, Jayaratne (1998b) performed a series of laboratory experiments in which rime density increased but he found no influence on charge sign. Nevertheless, the Avila *et al.* (1998, 1999) results showing that larger droplets can favour rimer negative charging will be associated with increased rime density. Thus surface roughness will affect charge transfer; however, in the present work, the droplet cloud spectrum was not a variable in the experiments and throughout, the velocity of the crystal stream past the target was 6 m s^{-1}. So, rime density itself was not a significant variable in the present studies.

(e)   The charge transfer mechanism

The relative growth rate theory (RGR) has its origins in the often observed result that growing ice surfaces charge positively, while sublimating ice surfaces charge negatively (Findeisen 1940; Findeisen and Findeisen 1943; Buser and Aufdermaur 1977; Marshall *et al.* 1978; Gaskell and Illingworth 1980; Jayaratne *et al.* 1983; Rydock and Williams 1991; Caranti *et al.* 1991; Dong and Hallett 1992; Saunders *et al.* 1993; Mason and Dash 2000). Most of those experiments were carried out by artificially cooling or heating an ice surface while its surface is removed by collisions or by fragmentation.

Consideration of the surface state of the other ice particle involved, the ice crystal, led Baker *et al.* (1987) to formulate the RGR hypothesis, which states that the ice surface growing faster by diffusion charges positively during an ice/ice collision and separation. The theory was developed by Baker and Dash (1994) in terms of a quasi-liquid layer on the ice surfaces; the surface layers are hypothesized to carry negative charges (Takahashi 1969; Caranti and Illingworth 1980) that are transferred together with mass during contact. Experiments by Mason and Dash (2000), in which ice surfaces experiencing growth or sublimation were brought into contact on a sensitive balance, related the charge and mass transferred. The more rapidly growing surface (artificially cooled in their experiments) was found to charge positively and the charge was carried in the mass transferred. However, the mass transfer was from the warmer to the colder ice surface: this result appears to conflict with the hypothesis of negative charge transfer from the faster to the slower growing surface. A solution was proposed by Dash *et al.* (2001)

involving collisional melting: the colder particle, the faster growing crystal, carries a higher negative surface charge density than the warmer graupel, but the colder crystal suffers less collisional melting, thus provides less liquid to transport the charge than the warmer graupel surface. When the particles separate, the colder crystal comes away with some of the warmer graupel mass but loses less negative charge, so charges positively. This argument does not work in reverse for positive rime charging because the crystal will always be colder than riming graupel. However, Mason and Dash (2000) could not investigate the case of a riming ice surface in which extra vapour and hence negative charge would be available to the rimer surface. So, we can hypothesize that in this case, the negative charge and mass are transferred in the same direction in order to account for positive rimers.

(f)   Resolution of effects of experimental differences

(i)   *Upper charge-sign reversal line.* It is clear that there are marked differences in the characteristics of the charge-sign regimes on an *EW* vs. *T* plot, as seen in Fig. 13. The low *EW* reversal line is obtained in one-cloud experiments whereas the higher lines were noted in two-cloud experiments. Considering the regions of the charge-sign reversal lines showing a negative to positive transition on increase in *EW*, the reversal line of Takahashi (1978) appears to match the two-cloud category of experiments, which lends circumstantial evidence to the suggestion that, in effect, those experiments were also of a two-cloud nature. The droplet source was either from an external chamber, or vapour was provided by a boiler in the main chamber; in both cases the droplets appeared in the chamber directly beneath the riming target. The ice crystals were nucleated and grew at the edges of the main chamber and from there were drawn into the droplet stream on the way to the rimer. Given that the crystals were nucleated continuously by pellets of dry ice in the chamber itself, the high concentration of crystals generated would have been in competition for the available vapour. Then, mixing the crystals into the fresh droplet cloud on the way to the target would have caused a transient high growth rate, as in the present experiments, which favoured the negative charging of the rimer. In contrast, the experiments reported from the Manchester group using a single cloud chamber consistently found a charge-sign reversal line at lower values of *EW*, indicating no transient mixing conditions in those experiments.

(ii)   *Sign of rimer charge above about −10 °C.* The one-cloud experiments show a negative rimer charge zone at low *EW* and high temperatures whereas the two-cloud experiments have all-positive rimers above about −10 °C (Fig. 13). Included in the category of two-cloud experiments are the studies of Berdeklis and List (2001) who also used two separate cloud chambers to produce crystals and droplets. Their values of *EW* did not extend to sufficiently high values to enable study of the upper charge-sign reversal line, although they did observe that the riming target charged positively at all temperatures above about −10 °C in agreement with Takahashi (1978), Pereyra *et al.* (2000) and the present two-cloud study. Furthermore, Takahashi (2002) revisited the subject and grew ice crystals in a separate chamber before mixing them into a droplet cloud on the way to a levitated ice target. Although high values of *EW* were not used, the rimer charged positively at temperatures above about −10 °C, confirming the effective two-cloud nature of those experiments. Gaskell and Illingworth (1980) mixed 100 μm frozen ice spheres into a droplet stream before encountering a riming target and noted positive target charging above −10 °C and negative below.

In one-cloud experiments, Saunders *et al.* (2001) showed that the introduction of extra water vapour to the riming target prompted positive charging; its increased growth

rate is consistent with the RGR hypothesis. This positive target result suggests that the supersaturation in the droplet cloud in the two-cloud experiments is higher than in the one-cloud experiments. In the one-cloud case the ice crystals deplete the droplet cloud and reduce the supersaturation; in contrast, in the two-cloud case the absence of crystals in the droplet cloud reduces the competition for vapour in the droplet cloud so that vapour is available for rimer diffusional growth favouring positive charging. In all cases, at lower temperatures the shorter droplet freezing times reduce the available vapour to the rimer surface and so permit negative charging, in accord with the RGR concept of Baker *et al.* (1987). The positive charging at low *EW*, noted in the two-cloud experiments (Fig. 13), is attributable to the same cause, namely the higher supersaturation in the droplet cloud when ice crystals are not present to use up the available water vapour.

5. CONCLUSIONS

Williams (2001) noted that the differences in laboratory results between Takahashi (1978) and Saunders *et al.* (1991) had not been resolved at that time, thus holding up a resolution of the issue of the charge transfer mechanism. The present study has offered a possible resolution of these differences with a solution linked to the heart of the charge transfer process and the controlling influence of relative diffusional growth rates influenced by local cloud supersaturations. The presence of supercooled water in the cloud influences the rime temperature through accretional heating, but is also indicative of water supersaturation conditions such that the ice surfaces grow by diffusion leading to substantial charge transfer.

The present data were obtained by mixing ice crystals grown in one cloud chamber, having a limited vapour supply, with supercooled droplets from a second chamber where they experienced no competition for vapour. The two clouds were mixed on their way to a riming target representing a falling graupel pellet and the charge sign during ice crystal rebounds was detected. The mixing time was sufficiently short that the ice crystals had insufficient time to increase their temperature to the appropriate value for their enhanced growth in the higher supersaturation. The continually replenished droplet cloud is above water saturation while the crystal cloud, because of competition for the limited vapour available, is subsaturated with respect to water, but supersaturated with respect to ice.

The conclusion of these experiments is that the conditions needed for the negative charging of graupel at high values of *EW*, shown by the upper boundaries of the sets of experiments represented in Fig. 13, have been identified. The ice crystals need to grow in a low supersaturation cloud before introduction to high supersaturation conditions leading to increased crystal growth rate just before impacting the riming target. The interpretation is consistent with the relative growth rate hypothesis that associates the faster growing particle with positive charging. The implications of these laboratory results to thunderstorm electrification require further analysis. A sheared situation involving particles from different environments falling through each other is likely to be associated with transients and so could lead to more negative rimers. On the other hand, the steady-state more vertical storms, the normal thunderstorm, will have time for the particles to be in a pseudo-steady state with no transients.

During precipitation growth in thunderstorms, both ice crystals and growing graupel pellets will be present in the updraught. When the graupel has grown sufficiently to have a fall velocity relative to the ice crystals, charge transfer events will occur. This is one situation represented by studies in which the interacting particles have had time to come to a steady growth state in their environment and may be represented by the Manchester data obtained in a single laboratory cloud. When crystals are grown in

a limited vapour supply in cloud conditions below water saturation, then mixed into a droplet cloud, the crystals experience a transient supersaturation leading to a high growth rate. The crystals are warmed rapidly by their growth and reach a new growth situation within tens of milliseconds. However, if the crystals encounter a riming graupel pellet during their rapid growth state they will tend to charge the riming graupel pellet negatively. The concept of the relative diffusional growth rate, introduced by Baker *et al.* (1987) links the ice surface growing faster by diffusion with positive charging. The laboratory studies obtained with two clouds suggest that in order to apply the two-cloud non-equilibrium charging results we need a situation where slow-growing ice crystals in a low-supersaturated environment are entrained into a region of high supersaturation. This may occur when crystals have had their growth rate decreased following mixing into regions of drier air. Such crystals, when subsequently mixed into moister regions containing riming graupel pellets, will experience a transient condition leading to enhanced negative charging of the rimer. Whether or not the two-cloud results apply depends on the mixing time; too long a time and thermal equilibrium will take place following mixing before the particles interact. Such cases may be associated with sheared clouds where falling precipitation particles fall from one environment through a boundary transition layer into a region of different origin and characteristics. The observation by Dye *et al.* (1986, 1988) of charge transfer interactions at the up/downdraught interface may apply here too.

There are two distinct sets of results that may be used appropriately to determine the graupel charge sign in thunderstorms. The early data from Manchester used a single chamber to create supercooled droplets and ice crystals in which the cloud particles involved grew in the same cloud as the graupel target: the cloud is supersaturated with respect to water and the crystals, droplets and target surface are in a steady-state growth situation. This condition may apply in clouds with a steady, vertical updraught in which graupel grows by accretion while smaller ice crystals are carried in the updraught. The results from the two-cloud studies show the effect of mixing growing ice crystals from an environment below water saturation into a growing droplet cloud. The crystals experience an enhanced growth rate that favours the negative charging of graupel. This case may be relevant to regions of clouds where entrainment has reduced the cloud supersaturation; subsequent mixing of particles from regions with differing saturation values will lead to transient growth that may influence the charge sign during crystal/graupel collisions. According to Lasher-Trapp *et al.* (2005), considerations of mixing processes in warm cumulus clouds for droplets experiencing entrainment leads them to experience different supersaturation histories during their transit through the cloud. The authors modelled the turbulent trajectories of droplets through cloud kinematic and thermodynamic fields and noted the sensitive dependence of droplet growth on the nature and time-scale of the mixing process. Similar entrainment and mixing with varying supersaturation histories will also apply to particles in the ice phase that may influence charge transfer during particle collisions. In particular, the predicted broadening of the spectrum implies that larger ice crystals grow faster under these turbulent conditions; the effect on charge transfer will be to promote the negative charging of graupel. There is scope here for further theoretical and laboratory study into the effects of mixing processes on the ice phase and electrification in clouds.

REFERENCES

Avila, E. E. and Caranti, G. M.	1994	A laboratory study of static charging by fracture in ice growing by riming. *J. Geophys. Res.*, **99,** 10611–10620
Avila, E. E., Aguirre Varela, G. G. and Caranti, G. M.	1995	Temperature dependence of static charging in ice growing by riming. *J. Atmos. Sci.*, **52,** 4515–4522
	1996	Charging in ice–ice collisions as a function of the ambient temperature and the larger particle average temperature. *J. Geophys. Res.*, **101,** 29609–29614
Avila, E. E., Caranti, G. M., Castellano, N. E. and Saunders, C. P. R.	1998	Laboratory studies of the influence of cloud droplet size on charge transfer during crystal–graupel collisions. *J. Geophys. Res.*, **103,** 8985–8996
Avila, E. E., Castellano, N. E. and Saunders, C. P. R.	1999	Effects of cloud-droplet spectra on the average surface-temperature of ice accreted on fixed cylindrical collectors. *Q. J. R. Meteorol. Soc.*, **125,** 1059–1074
Baker, B., Baker, M. B., Jayaratne, E. R., Latham, J. and Saunders, C. P. R.	1987	The influence of diffusional growth rates on the charge transfer accompanying rebounding collisions between ice crystals and soft hailstones, *Q. J. R. Meteorol. Soc.*, **113,** 1193–1215
Baker, M. B. and Dash, J. G.	1994	Mechanism of charge transfer between colliding ice particles in thunderstorms. *J. Geophys. Res.*, **99,** 10621–10626
Berdeklis, P. and List, R.	2001	The ice crystal–graupel collision charging mechanism of thunderstorm electrification. *J. Atmos. Sci.*, **58,** 2751–2770
Blyth, A. M. and Latham, J.	1993	Development of ice and precipitation in New Mexican summertime cumulus clouds. *Q. J. R. Meteorol. Soc.*, **119,** 91–120
Brooks, I. M., Saunders, C. P. R., Mitzeva, R. P. and Peck, S. L.	1997	The effect on thunderstorm charging of the rate of rime accretion by graupel. *Atmos. Res.*, **43,** 277–295
Buser, O. and Aufdermaur, A. N.	1977	Electrification by collision of ice particles on ice or metal targets. In *Electrical processes in atmospheres.* Eds. H. Delezalek and R. Reiter. Steinkopf, Darmstadt, West Germany
Caranti, G. M. and Illingworth, A. J.	1980	Surface potentials of ice and thunderstorm charge separation. *Nature*, **284,** 44–46
Caranti, G. M., Avila, E. E. and Ré, M. A.	1991	Charge transfer during individual collisions in ice growing from vapor deposition. *J. Geophys. Res.*, **96,** 15365–15375
Castellano, N. E., Avila, E. E. and Saunders, C. P. R.	2004	Theoretical model of the Bergeron–Findeisen mechanism of ice crystal growth in clouds. *Atmos. Env.*, **38,** 6751–6761
Dash, J. G., Mason, B. L. and Wettlaufer, J. S.	2001	Theory of charge and mass transfer in ice–ice collisions. *J. Geophys. Res.*, **106,** 20395–20402
Dong, Y. and Hallett, J.	1992	Charge separation by ice and water drops during growth and evaporation. *J. Geophys. Res.*, **97,** 20361–20371
Dye, J. E., Jones, J. J., Winn, W. P., Cerni, T. A., Gardiner, B., Lamb, D., Pitter, R. L., Hallett, J. and Saunders, C. P. R.	1986	Early electrification and precipitation development in a small, isolated Montana cumulonimbus. *J. Geophys. Res.*, **91,** 1231–1247
Dye, J. E., Jones, J. J., Weinheimer, A. J. and Winn, W. P.	1988	Observations within two regions of charge during initial thunderstorm electrification. *Q. J. R. Meteorol. Soc.*, **114,** 1271–1290
Dye, J. E., Winn, W. P., Jones, J. J. and Breed, D. W.	1989	The electrification of New Mexico thunderstorms. 1. Relationship between precipitation development and the onset of electrification. *J. Geophys. Res.*, **94,** 8643–8656
Findeisen, W.	1940	Über die Entstehung der Gewitterelektrizität. *Meteorol. Zeit.*, **57,** 201–215
Findeisen, W. and Findeisen, E.	1943	Investigations on the ice splinter formation on rime layers (A contribution to the origin of storm electricity and to the microstructure of cumulonimbi). *Meteorol. Zeit.*, **60**(5)
Gaskell, W. and Illingworth, A. J.	1980	Charge transfer accompanying individual collisions between ice particles and its role in thunderstorm electrification. *Q. J. R. Meteorol. Soc.*, **106,** 841–854
Heymsfield, A. J.	1982	A comparative study of the rates of development of potential graupel and hail embryos in High Plains storms. *J. Atmos. Sci.*, **39,** 2867–2897
Heymsfield, A. J. and Hjelmfelt, M. R.	1984	Processes of hydrometeor development in Oklahoma convective clouds. *J. Atmos. Sci.*, **41,** 2811–2835
Heymsfield, A. J. and Kajikawa, M.	1987	An improved approach to calculating terminal velocities of plate-like crystals and graupel. *J. Atmos. Sci.*, **44,** 1088–1099

Illingworth, A. J. and Lees, M. I. 1992 'Comparison of polarisation radar observations of clouds and lightning location data'. In Proc. 9th Int. Conf. Atmospheric Electricity, 15–19 June 1992, St. Petersburg, Russia

Jayaratne, E. R. 1998a Possible laboratory evidence for multipole electric charge structures in thunderstorms. *J. Geophys. Res.*, **103**, 1871–1878

1998b Density and surface temperature of graupel and the charge separation during ice crystal interactions. *J. Geophys. Res.*, **103**, 13957–13961

Jayaratne, E. R. and Saunders, C. P. R. 1985 Thunderstorm electrification: The effect of cloud droplets. *J. Geophys. Res.*, **90**, 13063–13066

Jayaratne, E. R., Saunders, C. P. R. and Hallett, J. 1983 Laboratory studies of the charging of soft-hail during ice crystal interactions. *Q. J. R. Meteorol. Soc.*, **109**, 609–630

Keith, W. D. and Saunders, C. P. R. 1990 Further laboratory studies of the charging of graupel during ice crystal interactions. *Atmos. Res.*, **25**, 445–464

Korolev, A. V., Isaac, G. A., Mazin, I. P. and Barker, H. W. 2001 Microphysical properties of continental clouds from *in situ* measurements. *Q. J. R. Meteorol. Soc.*, **127**, 2117–2151

Krehbiel, P. R. 1986 The electrical structure of thunderstorms. Pp. 90–113 in *The Earth's electrical environment*. Studies in Geophysics. National Academy Press, USA

Lasher-Trapp, S. G., Cooper, W. A. and Blyth, A. M. 2005 Broadening of droplet size distributions from entrainment and mixing in a cumulus cloud. *Q. J. R. Meteorol. Soc.*, **131**, 195–220

López, R. E. and Aubagnac, J.-P. 1997 The lightning activity of a hailstorm as a function of changes in its microphysical characteristics inferred from polarimetric radar observations. *J. Geophys. Res.*, **102**, 16799–16813

Macklin, W. C. 1962 The density and structure of ice formed by accretion. *Q. J. R. Meteorol. Soc.*, **88**, 30–50

Macklin, W. C. and Payne, G. S. 1967 A theoretical study of the ice accretion process. *Q. J. R. Meteorol. Soc.*, **93**, 195–213

Magono, C. and Takahashi, T. 1963 Experimental studies on the mechanism of electrification of graupel pellets. *J. Meteorol. Soc. Jpn*, **41**, 197–210

Marshall, B. J. P., Latham, J. and Saunders, C. P. R. 1978 A laboratory study of charge transfer accompanying the collision of ice crystals with a simulated hailstone. *Q. J. R. Meteorol. Soc.*, **104**, 163–178

Marshall, J. S. and Langleben, M. P. 1954 A theory of snow-crystal habit and growth. *J. Met.*, **11**, 104–120

Mason, B. L. and Dash, J. G. 2000 Charge and mass transfer in ice–ice collisions: Experimental observations of a mechanism in thunderstorm electrification. *J. Geophys. Res.*, **105**, 10185–10192

Mitzeva, R. P., Tsenova, B. and Saunders, C. P. R. 2005 A modelling study of the effect of cloud saturation and particle growth rates on charge transfer in thunderstorm electrification. *Atmos. Res.*, **76**, 206–221

Pereyra, R. G., Avila, E. E., Castellano, N. E. and Saunders, C. P. R. 2000 A laboratory study of graupel charging. *J. Geophys. Res.*, **105**, 20803–20812

Reynolds, S. E. and Brook, M. 1956 Correlation of the initial electric field and the radar echo in thunderstorms. *J. Met.*, **13**, 376–380

Reynolds, S. and Neil, H. W. 1955 The distribution and discharge of thunderstorm charge-centers. *J. Met.*, **12**, 1–12

Reynolds, S., Brook, M. and Gourley, M. F. 1957 Thunderstorm charge separation. *J. Met.*, **14**, 426–436

Rust, W. D. and MacGorman, D. R. 2002 Possibly inverted-polarity electrical structures in thunderstorms during STEPS. *Geophys. Res. Lett.*, **29**, 1571, doi: 10.1029/2001GL014303

Rust, W. D., MacGorman, D. R., Bruning, E. C., Weiss, S. A., Krehbiel, P. R., Thomas, R. J., Rison, W., Hamlin, T. and Harlin, J. 2005 Inverted-polarity electrical structures in thunderstorms in the Severe Thunderstorm Electrification and Precipitation Study (STEPS). *Atmos. Res.*, **76**, 247–271

Rydock, J. P. and Williams, E. R. 1991 Charge separation associated with frost growth. *Q. J. R. Meteorol. Soc.*, **117**, 409–420

Saunders, C. P. R. and Peck, S. L. 1998 Laboratory studies of the influence of the rime accretion rate on charge transfer during crystal/graupel collisions. *J. Geophys. Res.*, **103**, 13949–13956

Saunders, C. P. R., Keith, W. D. and Mitzeva, R. P. 1991 The effect of liquid water on thunderstorm charging. *J. Geophys. Res.*, **96**, 11007–11017

Saunders, C. P. R., Hickson, M., Malone, M. D. and von Richtofen, J.	1993	Charge separation during the fragmentation of rime and frost. *Atmos. Res.*, **29,** 261–270
Saunders, C. P. R., Avila, E. E., Peck, S. L., Castellano, N. E. and Aguirre Varela, G. G.	1999a	A laboratory study of the effects of rime ice accretion and heating on charge transfer during ice crystal/graupel collisions. *Atmos. Res.*, **51,** 99–117
	1999b	'Vapor and heat supply to riming graupel: effect on charging'. Pp. 268–271 in Proc. 11th Int. Conf. Atmospheric Electricity, 7–11 June 1999, Guntersville, Alabama, USA
Saunders, C. P. R., Peck, S. L., Aguirre Varela, G. G., Avila, E. E. and Castellano, N. E.	2001	A laboratory study of the influence of water vapour and mixing on the charge transfer process during collisions between ice crystals and graupel. *Atmos. Res.*, **58,** 187–203
Stolzenburg, M., Marshall, T. C. and Rust, W. D.	2001	Serial soundings of electric field through a mesoscale convective system. *J. Geophys. Res.*, **106,** 12371–12380
Takahashi, T.	1969	Electric potential of liquid water on an ice surface. *J. Atmos. Sci*, **26,** 1253–1258
	1978	Riming electrification as a charge generation mechanism in thunderstorms. *J. Atmos. Sci.*, **35,** 1536–1548
Takahashi, T. and Miyawaki, K.	2002	Reexamination of riming electrification in a wind tunnel. *J. Atmos. Sci.*, **59,** 1018–1025
Williams, E. R.	1989	The tripole structure of thunderstorms. *J. Geophys. Res.*, **94,** 13151–13167
	2001	The electrification of severe storms. Ch. 13, pp. 527–561 in *Severe convective storms*. Ed. C. A. Doswell III. AMS Meteorol. Monograph Series, 28
Williams, E. R. and Zhang, R.	1996	Density of rime in laboratory simulations of thunderstorm microphysics and electrification. *J. Geophys. Res.*, **101,** 29715–29719
Williams, E. R., Zhang, R. and Rydock, J.	1991	Mixed-phase microphysics and cloud electrification. *J. Atmos. Sci.*, **48,** 2195–2203
Willis, P. T., Hallett, J., Black, R. A. and Hendricks, W.	1994	An aircraft study of rapid precipitation development and electrification in a growing convective cloud. *Atmos. Res.*, **33,** 1–24